THE JOURNAL OF PHYSICAL CHEMISTRY A

Article

pubs.acs.org/JPCA

Chalcogen Bonding between Tetravalent SF_4 and Amines

Vincent de Paul N. Nziko and Steve Scheiner*

Department of Chemistry and Biochemistry, Utah State University, Logan, Utah 84322-0300, United States

Supporting Information

ABSTRACT: The N···S chalcogen bond between SF_4 and a series of alkyl and arylamines is examined via ab initio calculations. This bond is a strong one, with a binding energy that varies from a minimum of 7 kcal/mol for NH_3 to 14 kcal/mol for trimethylamine. Its strength derives in large measure from charge transfer from the N lone pair into the σ^*(SF) antibonding orbitals involving the two equatorial F atoms, one of which is disposed directly opposite the N atom. Decomposition of the total interaction energy reveals that the induction energy constitutes more than half of the total attraction. The positive region of the molecular electrostatic potential of SF_4 that lies directly opposite the equatorial F atoms is attracted to the N lone pair, but the magnitude of this negative region on each amine is a poor predictor of the binding energy. The shortness and strength of the N···S bond in the dimethylamine···SF_4 complex suggest it may better be described as a weak covalent bond.

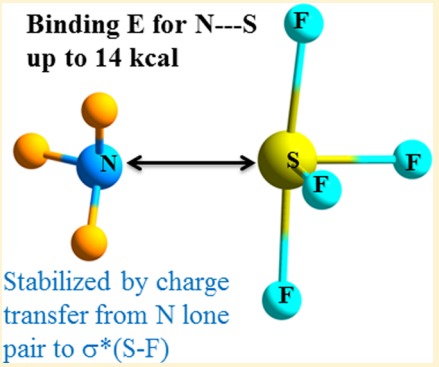

INTRODUCTION

Of the various noncovalent bonds, the H-bond is arguably the most important and prevalent. It is typically formulated as the positioning of two molecules such that the H atom of one molecule, A−H, acts as a bridge to an atom D of another molecule. Although its earliest conception applied highly electronegative atoms like O, F, and N as donor and acceptors,[1−3] a great deal of work since that time has broadened the picture to include other atoms such as C, S, and Cl.[4−13] In addition, the proton need not interact with a lone pair of the acceptor atom but also with other electron sources such as the π-systems of unsaturated molecules.

It is not only a proton that can serve as a bridge between two molecules. The anisotropic charge distribution around halogen atoms (X) allow them to act in a similar capacity.[14−25] More specifically, there is a positive pole region directly along the extension of each R−X covalent bond, surrounded by an equator of negative charge. This positive region, commonly termed a σ-hole, is able to interact attractively with a negatively charged atom of another molecule. The stability of this halogen bond is augmented by charge transfer into the σ^*(RX) antibonding orbital, precisely analogous to the case of a H-bond. Like its congener H-bond, the halogen bond can also be quite strong. This phenomenon is not limited to halogen atoms, but a similar set of physical forces allow the much less electronegative pnicogen family (N, P, As, etc.) to participate in bonds of comparable strength and similar origin.[26−35]

Unsurprisingly, the chalcogen family is not excluded from this sort of noncovalent bonding. A chalcogen bond is formed when a member of this family of atoms (e.g., S or Se) engages in an attractive and direct noncovalent interaction with an electronegative atom like N or O.[36−44] The importance of chalcogen bonds has been underscored by their strength, which is comparable to and sometimes exceeds that of HBs. For instance, there is a direct interaction of S of FHS with N of NH_3, forming a strong S···N noncovalent bond[45] with a binding energy of 8 kcal/mol.

With respect to S, prior study of its chalcogen bonding has centered around the divalent bonding situation, e.g., SO_2, HSF, thioethers, or thiazole nucleosides.[30,41,46−53] Unlike its congener O, the S atom commonly engages in higher order bonding, as, for example, the tetravalent S in H_2SO_4 or SF_4.

The present study is thus meant to fill this gap in our present knowledge about S chalcogen bonding. SF_4 is taken as the prototypical tetravalent S molecule. Experimentally, SF_4 is widely used in fluorination of alcohols, aldehydes, ketones, and carboxylic acids.[54,55] SF_4 is reacted with primary amines to yield sulfur difluoro imide and sulfur diimides. Although alternative methods for the synthesis of these compounds exist, the most common one is the reaction[56−58] of compounds containing the primary amino group (NH_2) with SF_4. This tetravalent S is allowed to interact with a series of electron donor amines, covering a range of both alkylamines and N-containing heteroaromatic rings. It is found that the S···N chalcogen bonds are all quite strong, greater in magnitude than the prototypical H-bond within a water dimer. Indeed, the binding energy ranges up to as much as 14 kcal/mol, so that some of these interactions may be considered as having crossed the threshold from noncovalent to weak covalent S−N bond.

COMPUTATIONAL PROCEDURES

Calculations were carried out with the Gaussian09 program.[59] Geometries were fully optimized at the MP2/aug-cc-pVDZ level. This method has demonstrated its reliability for a range of

Received: September 11, 2014
Revised: October 20, 2014
Published: October 22, 2014

 © 2014 American Chemical Society

noncovalent interactions.[17,26,60−65] Harmonic vibrational frequencies verified the characterization of minima. The binding energy, E_b, was calculated as the difference between the total energy of the complex and the sum of the isolated optimized monomers. Interaction energy ΔE was defined relative to the monomers in their geometries within the context of the complex. Basis set superposition error (BSSE) was corrected via the counterpoise technique.[66] Molecular electrostatic potentials (MEPs) were calculated on the electron density isosurface of 0.001 au and extrema evaluated using the WFA-SAS program.[67] The interaction energy was dissected using SAPT methodology.[68] The SAPT0 calculations[68,69] were carried out at the HF/cc-pVDZ computational level, using the MOLPRO program.[70] The Natural Bond Order (NBO) method[71,72] was used to evaluate charge transfer effects using the NBO-3 program, incorporated in the Gaussian09 program.

RESULTS

The optimized structure of $H_3N\cdots SF_4$ is illustrated in Figure 1, which is representative of all of these heterodimers involving an

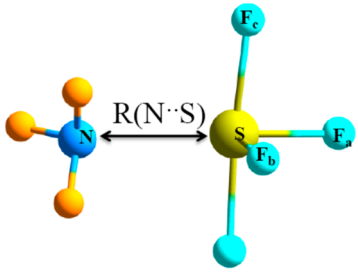

Figure 1. Atomic labeling used to define geometries of complexes of amines with SF_4.

alkylamine. F_a and F_b are the equatorial F atoms, with F_a lying nearly opposite the N atom, F_c represents one of the two symmetrically disposed axial F atoms. The first row of Table 1 indicates the binding energy grows rapidly as methyl groups are added, from a minimum of 6.62 kcal/mol for NH_3 and peaking at 14.39 kcal/mol for trimethylamine (TMA). The enhanced strength arising from each methyl addition is consistent with the idea that alkyl groups are electron-releasing, and can hence facilitate the donation of electron charge from the amine. The next row shows a corresponding contraction of the intermolecular separation with each succeeding increase in binding energy, with the exception of a small increase for TMA. The N atom sits nearly exactly opposite one of the two equatorial F atoms of SF_4, with a $\theta(N\cdots SF_a)$ angle within 10° of 180°. Concomitant with the binding, there is a stretch in this $S-F_a$ bond, between 18 and 66 mÅ, and this stretch correlates with the overall binding energy. The other equatorial $S-F_b$ and axial $S-F_c$ bonds also undergo a stretch, albeit not quite as large. The full thermodynamic quantities in the remaining rows of Table 1 indicate that the zero-point vibrational energies introduce a small decrease in the magnitude of ΔE on going to ΔH. When the entropic loss is factored in, ΔG hovers around zero (slightly positive for the three most weakly bound complexes and slightly negative for TMA), suggesting the presence of the dimer even at room temperature.

A similar sort of analysis was also carried out for a set of N-containing heteroaromatics shown in Figure 2. Pyridine is a six-

Figure 2. Heteroaromatic amines, (a) pyridine, (b) pyrazine, (c) pyridazine, (d) pyrimidine, and (e) imidazole, used in this study.

membered ring containing a single N. Pyrazine, pyridazine, and pyrimidine add a second N to the ring, in the 1,4, 1,2, and 1,3 positions, respectively. Imidazole retains two N atoms but reduces the ring size to five atoms. The properties of their complexes with SF_4 are reported in Table 2 where it may first be noted that the binding energies all vary within the relatively narrow range of 7.4 to 9.4 kcal/mol. This range makes these complexes intermediate in strength between NH_3 and

Table 2. Energetic (kcal/mol) and Geometric Aspects of Heteroaromatic Amine:SF_4 Complexes

	pyridine	pyrazine	pyridazine	pyrimidine	imidazole
E_b	−9.39	−7.69	−8.62	−7.43	−9.14
$R(N\cdots S)$ (Å)	2.308	2.372	2.338	2.416	2.285
$\theta(N\cdots SF_a)$ (deg)	171.9	172.5	173.7	173.1	172.3
$\Delta r(S-F_a)$ (mÅ)	43.3	31.1	32.4	27.1	43.9
$\Delta r(S-F_b)$ (mÅ)	15.5	11.5	23.7	9.0	14.6
$\Delta r(S-F_c)$ (mÅ)	41.7	36.6	31.4	38.3	37.5
ΔH (298 K)	−8.24	−6.46	−7.25	−6.23	−7.90
ΔS^a (cal mol^{-1} K^{-1})	−33.01	−37.03	−30.46	−31.03	−35.35
ΔG (298 K)	2.76	4.18	3.07	4.16	2.65

[a]Evaluated at 25 °C.

Table 1. Energetic (kcal/mol) and Geometric Aspects of Alkylamine:SF_4 Complexes

	ammonia	methylamine	dimethylamine	trimethylamine
E_b	−6.62	−9.72	−13.25	−14.39
$R(N\cdots S)$ (Å)	2.571	2.188	2.158	2.227
$\theta(N\cdots SF_a)$ (deg)	173.3	170.3	169.7	171.3
$\Delta r(S-F_a)$ (mÅ)	18.5	52.9	65.9	62.4
$\Delta r(S-F_b)$ (mÅ)	8.7	27.9	36.9	32.4
$\Delta r(S-F_c)$ (mÅ)	22.7	43.3	43.7	45.2
ΔH (298 K)	−5.26	−8.32	−11.63	−12.66
ΔS^a (cal mol^{-1} K^{-1})	−27.00	−36.38	−39.44	−40.36
ΔG (298 K)	2.80	2.47	0.12	−0.63

[a]Evaluated at 25 °C.

dx.doi.org/10.1021/jp509212t | J. Phys. Chem. A 2014, 118, 10849−10856

CH_3NH_2. Pyridine forms the strongest complex, followed by the disubstituted rings, of which pyridazine with its adjacent N atom forms the strongest. The five-membered ring of imidazole is stronger still, despite the presence of two N atoms. Like the binding energies, the intermolecular R(N···S) distances are also fairly similar to one another, with the general trend of shorter distances associated with strong bonds. Also like the alkylamines, the S−F bonds elongate upon formation of each complex. ΔH lies in the range between −6.2 and −8.2 kcal/mol, while ΔG is positive, between 2.7 and 4.2 kcal/mol.

Energy Decomposition. The total interaction energy in each of these dimers was dissected via SAPT to provide the various attractive and repulsive components. These quantities are displayed graphically in Figure 3 from which one can

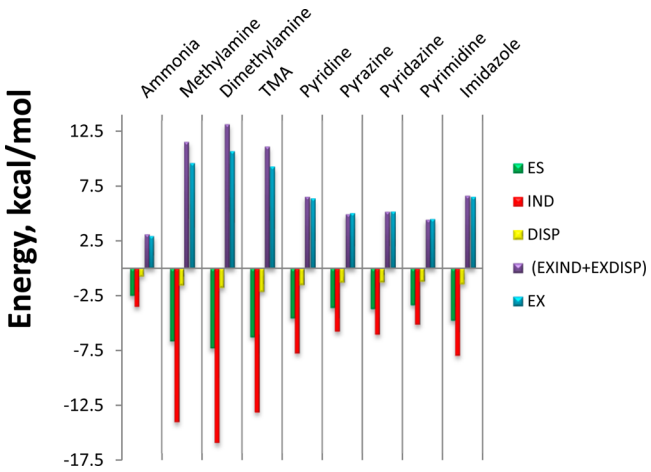

Figure 3. SAPT components of interaction energy of indicated amine with SF_4.

quickly see their relative magnitudes. It is immediately clear that induction makes the largest contribution to the binding followed by electrostatic and then dispersion. The magnitudes of these quantities vary from one system to the next, but their relative proportions are surprisingly constant. Specifically, the induction accounts for more than half of the total attractive force (52−63%), compared to 29−37% arising from electrostatics, and 8−12% from dispersion.

It is instructive to compare the total interaction energy as calculated by SAPT and that from MP2, with appropriate counterpoise correction. The SAPT values are displayed in Figure 4 as the solid blue line. The MP2 binding energies from

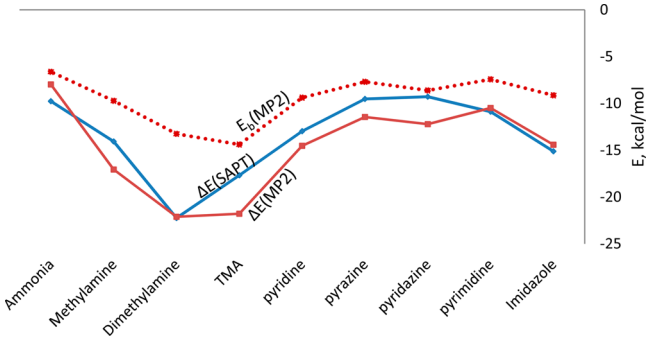

Figure 4. Interaction energies of amines with SF_4 calculated by SAPT (blue) and MP2 (red). Broken red line refers to binding energy at MP2 level.

Tables 1 and 2 are indicated by the broken red curve, but it must be recalled that these two quantities correspond to different properties. The binding energy E_b makes reference to the monomers in their optimized geometries, whereas the interaction energy ΔE is calculated with respect to the monomers in their geometries within the context of the complex. E_b and ΔE thus differ by what is sometimes termed the "distortion energy", the energy required for the monomers to alter their geometry from their optimized structure to that within the complex. Since the SAPT quantities refer to ΔE, the distortion energy is removed from the MP2 quantities, thereby presenting the MP2 values of ΔE as the solid red curve in Figure 4, so as to facilitate a valid comparison.

One may observe first that the distortion energy, the difference between the solid and broken red curves in Figure 4, is fairly small for NH_3, but grows as methyl groups are added. The heteroaromatics also present a fairly large, but nearly uniform distortion energy, most notably imidazole where it is 5.3 kcal/mol. Turning next to the comparison between SAPT and MP2, the solid red and blue curves are fairly similar. The largest difference occurs for $(CH_3)_3N$, which is perhaps a product of the steric repulsion between the three methyl groups and the F atoms and the S lone pair of SF_4.

The importance of induction as well as electrostatics is also underscored by their ability to predict the total interaction energy. IND is linearly related to the full SAPT interaction energy, with a correlation coefficient R^2 of 0.88, as is ES. The correlation improves when these two components are compared with the MP2 values of ΔE, with R^2 = 0.95. Although small in magnitude, DISP also scales linearly with ΔE, with R^2 = 0.97.

Comparison of Tetravalent with Divalent S. As this work represents the first examination of the chalcogen bonds formed by tetravalent S, it would be informative to draw a comparison with the more common divalent S. The properties of the complexes formed by SF_4 with both NH_3 and trimethylamine are displayed in Table 3 and are compared

Table 3. Properties of Divalent and Trivalent S Complexes

complex	E_b (kcal/mol)	R(N···S) (Å)	θ(FS···N) (deg)
FHS···NH_3	−7.92	2.466	171.0
F_2S···NH_3	−6.95	2.480	173.0
F_4S···NH_3	−6.62	2.573	173.3
FHS···TMA	−14.56	2.183	170.6
F_2S···TMA	−14.48	2.158	172.3
F_4S···TMA	−14.39	2.227	171.3

with those in which SF_4 is replaced by both H_2S and HSF. The first three rows of the table indicate the strong similarities of the three complexes involving NH_3, with a small advantage for FHS. Adding three methyl groups to the amine approximately doubles the strength of the interaction, but shows even less of a distinction between the divalent and tetravalent S complexes, even though the intermolecular distance is slightly longer in the latter case.

Molecular Electrostatic Potentials. With regard to the electrostatic segment of the interaction energy, examination of the molecular potentials of the various electron donors all show a negative region in the vicinity of the N atoms. These regions can be quantitatively assessed via the value of the most negative point on a surface that corresponds to an isodensity contour of 0.001 au. The values of this quantity, $V_{s,min}$, are presented in the

dx.doi.org/10.1021/jp509212t | J. Phys. Chem. A 2014, 118, 10849−10856

first column of Table 4. The alkylamines in the first four rows show a diminishing trend as methyl groups are added. This

Table 4. Extrema in the Molecular Electrostatic Potentials (kcal/mol) on an Isodensity Surface Corresponding to 0.001 au

	$V_{s,min}$		$V_{s,max}$
NH_3	−39.39	H_2S	+42.15
methylamine	−38.04	FHS	+39.16
dimethylamine	−35.63	SF_4	+42.19
trimethylamine	−33.45		
pyridine	−29.76		
pyrazine	−23.10		
pyridazine	−25.45		
pyrimidine	−35.60		
imidazole	−36.27		

trend is opposite to the pattern of binding energies in Table 1 or even the ES terms in the SAPT decomposition. Within the context of the heteroaromatics, $V_{s,min}$ varies as pyrazine < pyridazine < pyridine < pyrimidine < imidazole, which again differs from the binding energies in Table 2, where, for example, pyrimidine is the most weakly bound and pyridine the strongest. In summary, then, $V_{s,min}$ is a poor indicator of binding strength or even of the electrostatic component.

On the positive side, MEPs do offer some insight into the similarity between divalent and tetravalent S with respect to its chalcogen bonding. The MEPs are illustrated in Figure 5 for

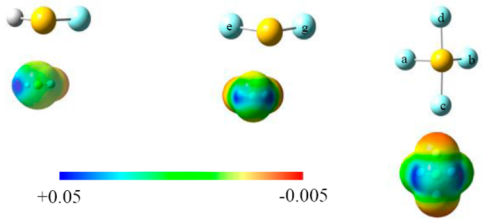

Figure 5. MEP of HSF, SF_2, and SF_4, all calculated on isodensity surface of ρ = 0.001 au.

divalent H_2S and FHS, followed by tetravalent SF_4. The similarities are evident. All potentials contain a red (negative) area along the extension of the S−F bonds, particularly the axial SF bonds of SF_4.

More importantly, there is a blue (positive) region near the S atom, along the extension of each F−S bond, a so-called σ-hole. Quantitation of this hole via an evaluation of $V_{s,max}$, the maximum of this potential on the ρ = 0.001 au isodensity contour, leads to the values reported in Table 4. It is immediately plain that the depth of this hole is nearly independent of the valency of the S atom. Whether H_2S, FSH, or SF_4, $V_{s,max}$ lies within the narrow range of 39 to 42 kcal/mol. It should be finally noted that there is no positive σ-hole opposite the axial F atoms of SF_4, due to the presence of one axial F atom directly opposite the other.

Charge Rearrangement. Treatment of the wave function via the NBO method leads to localized orbitals, which provide insights into the chemical nature of noncovalent interactions. In particular, the overlap of the N lone pair of the amine with the F_a−S σ^* antibonding orbital allows charge transfer/hyperconjugation from the former to the latter. This transfer has been shown to be a dominant factor in the formation of chalcogen bonds such as these. The magnitude of this transfer is listed in the first column of Table 5 as a perturbation energy

Table 5. NBO Second Order Perturbation Energy (kcal/mol) for Complexes with SF_4

	$E^a(2)^a$	$E^b(2)^b$	$E^a(2) + E^b(2)$	θ(N···SF_a) (deg)	θ(N···SF_b) (deg)
ammonia	14.68	3.70	18.48	173.3	77.4
methylamine	41.49	16.77	58.26	170.3	80.6
dimethylamine	NA[c]	NA[c]	NA[c]	169.7	81.2
trimethylamine	41.28	20.65	61.93	171.3	81.7
pyridine	36.57	11.79	48.36	171.9	80.2
pyrazine	27.76	8.13	36.89	172.5	79.5
pyridazine	27.80	9.60	37.4	173.7	80.4
pyrimidine	24.59	6.93	31.52	173.1	79.4
imidazole	37.10	9.46	46.56	172.3	80.6

[a]NBO perturbation energy corresponding to $N_{lp}\cdots\sigma^*(S-F_a)$. [b]NBO perturbation energy corresponding to $N_{lp}\cdots\sigma^*(S-F_b)$. [c]The interaction is strong enough that NBO places a covalent bond between N and S, i.e., considers the entire system as one unit.

$E^a(2)$. This quantity is rather large, ranging from a minimum of 14.7 kcal/mol for NH_3 all the way up above 40 kcal/mol for methylamine and trimethylamine. The heteroaromatics also display large values of E(2), between 25 and 37 kcal/mol. Indeed, this interaction is so strong that in the case of dimethylamine, NBO assesses that there is a covalent bond linking the S and N atoms.

In a particularly interesting finding, the $\sigma^*(F_aS)$ antibonding orbital, for which F_a lies opposite the N atom, is not the only one that can accept charge. Its overlap with the N lone pair is obvious in Figure 6a, but one can see in Figure 6b that the same

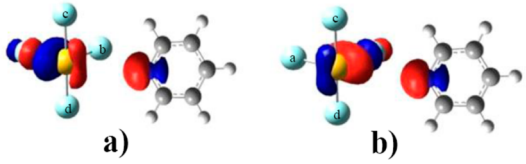

Figure 6. Overlap between NBO N lone pair orbital and (a) $\sigma^*(SF_a)$ and (b) $\sigma^*(SF_b)$.

N lone pair can also engage with $\sigma^*(F_bS)$ wherein F_b is the other equatorial F atom of SF_4. Whereas F_a lies nearly opposite the N lone pair, so the $\sigma^*(SF_a)$ orbital points directly at N, the roughly 80° θ(N···SF_b) angle reduces the overlap with this antibonding orbital. The amount of hyperconjugation associated with this second antibond is reported in the second column of Table 5 as $E^b(2)$ and can be as large as 50% of $E^a(2)$ ($N_{lp} \rightarrow \sigma^*(F_aS)$), so its effect cannot be ignored.

As a means of further probing the influence of the two SF antibonding orbitals, the SF_4 molecule was pivoted around the S−F_b axis by an angle φ, holding fixed the other geometrical parameters of the pyridine···SF_4 complex. On the basis of the diagrams in Figure 6, this rotation ought to have little effect upon the overlap between the N lone pair and the $\sigma^*(SF_b)$ orbital, but it would misalign the lone pair with $\sigma^*(SF_a)$. The values of E(2) computed during this rotation support this supposition. As may be seen in Figure 7, $E^b(2)$ remains nearly constant over a ±20° misalignment, while $E^a(2)$ suffers an erosion of some 16%.

dx.doi.org/10.1021/jp509212t | J. Phys. Chem. A 2014, 118, 10849−10856

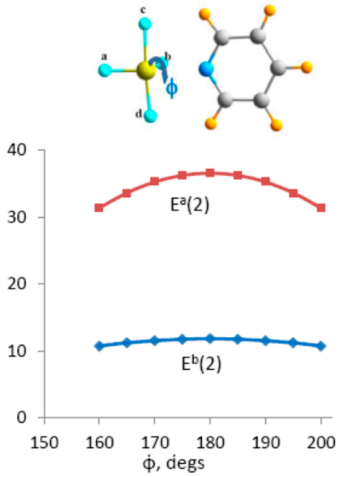

Figure 7. Variation of E(2) for transfer from N lone pair into $\sigma^*(SF_a)$ and $\sigma^*(SF_b)$ antibonding orbitals, as a function of rotation of SF_4 around S−F_b axis, $\varphi(N\cdots SF_bF_a)$.

In addition to the transfer from one specific localized orbital to another, there are charge rearrangements that involve the entire complex. The redistribution of total electron density that accompanies the formation of the $NH_3\cdots SF_4$ complex is displayed in Figure 8a where increases in density correspond

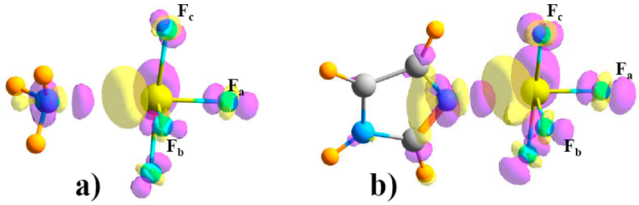

Figure 8. Rearrangement of electron density in (a) $NH_3\cdots SF_4$ and (b) imidazole$\cdots SF_4$ complexes. Purple and yellow regions correspond, respectively, to increases and decreases, and contours are ±0.003 au.

to purple and losses to yellow. One may note first that there is a charge buildup directly between the N and S atoms, in approximately the position of the center of what may be termed a noncovalent N···S bond. A larger yellow region of loss occurs immediately to the left of the S. This pattern is typical of halogen, chalcogen, and pnicogen bonds. A purple charge buildup may be noted behind the S atom, corresponding to a $\sigma^*(SF_b)$ antibonding orbital.

It is especially interesting to note that the four F atoms of SF_4 are all surrounded by a purple region of charge gain. This pattern does not much distinguish between the two equatorial F atoms whose $\sigma^*(SF)$ antibonding orbital accept charge from the amine and the axial F atoms that do not. Indeed, the NBO atomic charges of these F atoms all become more negative, as reported in Table 6. Figure 8b displays the charge redistribution of the imidazole$\cdots SF_4$ complex, which is very much like that for the simpler NH_3 amine. Again, all four SF_4 F atoms acquire additional density, which is verified by NBO atomic charges in Table 6. This pattern is in fact characteristic of all of the complexes examined here, whether alkylamine or heteroaromatic amine. This similarity in charge redistribution is also consistent with the observation that all four S−F bonds of SF_4 elongate upon formation of the complex. In fact, there is a fairly strong linear relationship between the change in charge on the F_a atom and its elongation, with a correlation coefficient R^2 of

Table 6. Changes in NBO Atomic Charges (me) within SF_4 That Occur upon Formation of Complex with Indicated Amine

	S	F_a	F_b	F_c
ammonia	3.18	−23.25	−10.78	−15.01
methylamine	−86.9	−65.45	−22.03	−21.61
dimethylamine	−97.41	−52.89	−26.11	−27.29
TMA	−81.91	−46.64	−23.57	−18.71
pyridine	−27.22	−41.83	−8.86	−21.01
pyrazine	−12.50	−31.01	−6.34	−19.09
pyridazine	−7.06	−33.69	−5.56	−15.28
pyrimidine	−5.36	−29.29	−6.15	−22.80
imidazole	−25.11	−38.60	−9.76	−29.32

0.955. In terms of the hyperconjugation, the strength of the S−F bond might be measured in terms of the populations of its σ and σ^* orbitals. Since the former would act to strengthen this bond, and σ^* to weaken it, the overall effect can be assessed as $(\sigma-\sigma^*)$. This population difference is also linearly related to $\Delta r(SF_a)$, with $R^2 = 0.945$. Correlations exist for the other S−F bond lengths as well, but are of poorer quality.

SUMMARY

All of the amines, both alkyl and heteroaromatic, engage in strong chalcogen-bonds with SF_4. The alkylamine binding is very sensitive to the number of methyl groups; binding energies vary from 6.6 kcal/mol for NH_3 to 14.4 kcal/mol for trimethylamine. Heteroaromatics are less sensitive to the nature of the ring, all binding in the range between 7 and 9 kcal/mol. In all cases, one of the equatorial S−F bonds is arranged directly opposite the approaching N atom. It is into this σ^*(S−F) antibonding orbital that the N lone pair transfers some of its charge, which acts as a strong stabilizing influence on the complex. There is a lesser, but significant, amount of charge that is deposited into the σ^*(S−F) antibonding orbital of the other equatorial F atom of SF_4. The associated induction energy is the largest contributor to the binding of these complexes, constituting more than half of the total attractive energy, followed by electrostatic and then dispersion energy.

Examination of the charge rearrangements that accompany formation of each complex shows that the charge transferred from the amine to the SF_4 molecule is ultimately distributed among all four F atoms, as well as the central S atom. The ensuing increase in the partial negative charge on these F atoms explains the elongation of the S−F bonds. The molecular electrostatic potentials surrounding each monomer furnish some useful information about the binding. For example, the N lone pair is attracted to a positive region of the SF_4 potential that lies directly opposite each of the equatorial F atoms. However, the quantitative assessment of the former negative N area is poorly correlated with the total interaction energy or even the full electrostatic component.

The especially strong interaction in the complex between dimethylamine and SF_4 leads to the conclusion that the N···S bond is approaching the regime where it might be better thought of as a covalent bond. The binding energy is 13 kcal/mol, and the R(N−S) distance is only 2.16 Å. The charge transferred from amine to SF_4 upon formation of this N−S bond is some 0.23 e, exceeding what is normally observed in a noncovalent bond.

There is experimental confirmation of some of our most important findings. SF_4 was found by a recent crystal structure

dx.doi.org/10.1021/jp509212t | J. Phys. Chem. A 2014, 118, 10849−10856

determination[73] to bind to an amine in the manner described here. In its complex with triethylamine, one of the equatorial F atoms of SF_4 lies 173° away from the N atom, within 2° of the structure described here with trimethylamine. Also quite similar is the R(N···S) distance of 2.38 Å, only slightly longer than the equivalent distance in our calculated TMA complex. Also confirmed by this crystal structure is the elongation of all of the S−F bonds upon formation of the complex.

There is an indication in the literature that a tetravalent S can engage in a chalcogen bond with an O atom as well. The complex between water and $SO_2(CH_3)_2$ contains what would appear at least geometrically to be a S···O chalcogen bond, of length 3.34 Å, and with the water O atom situated opposite one of the two O covalently bonded to S.[74] However, there was little analysis of the nature of any possible S···O bond; furthermore, the energy of this bond could not be disentangled from the combined effects of several H-bonds.

■ ASSOCIATED CONTENT

Ⓢ Supporting Information

Full references 59 and 70. This material is available free of charge via the Internet at http://pubs.acs.org.

■ AUTHOR INFORMATION

Corresponding Author

*E-mail: steve.scheiner@usu.edu.

Notes

The authors declare no competing financial interest.

■ ACKNOWLEDGMENTS

Computer, storage, and other resources from the Division of Research Computing in the Office of Research and Graduate Studies at Utah State University are gratefully acknowledged.

■ REFERENCES

(1) Joesten, M. D.; Schaad, L. J. *Hydrogen Bonding*; Marcel Dekker: New York, 1974; p 622.

(2) Schuster, P.; Zundel, G.; Sandorfy, C. *The Hydrogen Bond. Recent Developments in Theory and Experiments*; North-Holland Publishing Co.: Amsterdam, The Netherlands, 1976.

(3) Schuster, P. *Hydrogen Bonds*; Springer-Verlag: Berlin, Germany, 1984; Vol. *120*, p 117.

(4) Nishio, M.; Umezawa, Y.; Honda, K.; Tsuboyama, S.; Suezawa, H. CH/π Hydrogen Bonds in Organic and Organometallic Chemistry. *CrystEngComm* **2009**, *11*, 1757−1788.

(5) van der Veken, B. J.; Delanoye, S. N.; Michielsen, B.; Herrebout, W. A. A Cryospectroscopic Study of the Blue-Shifting C−H···O Bonded Complexes of Pentafluoroethane with Dimethyl Ether-D_6, Acetone-D_6 and Oxirane-D_4. *J. Mol. Struct.* **2010**, *976*, 97−104.

(6) Scheiner, S.; Gu, Y.; Kar, T. Evaluation of the H-Bonding Properties of CH···O Interactions Based Upon NMR Spectra. *J. Mol. Struct.* **2000**, *500*, 441−452.

(7) Karpfen, A.; Kryachko, E. S. The Dimers of Glyoxal and Acrolein with H_2O and HF: Negative Intramolecular Coupling and Blue-Shifted C−H Stretch. *Chem. Phys. Lett.* **2010**, *489*, 39−43.

(8) Gu, Y.; Kar, T.; Scheiner, S. Comparison of the CH···N and CH···O Interactions Involving Substituted Alkanes. *J. Mol. Struct.* **2000**, *552*, 17−31.

(9) Domagala, M.; Grabowski, S. J. Hydrocarbons as Proton Donors in C−H···N and C−H···S Hydrogen Bonds. *Chem. Phys.* **2010**, *367*, 1−6.

(10) Arunan, E.; Desiraju, G. R.; Klein, R. A.; Sadlej, J.; Scheiner, S.; Alkorta, I.; Clary, D. C.; Crabtree, R. H.; Dannenberg, J. J.; Hobza, P.; Kjaergaard, H. G.; Legon, A. C.; Mennucci, B.; Nesbitt, D. J. Definition of the Hydrogen Bond. *Pure Appl. Chem.* **2011**, *83*, 1637−1641.

(11) Latajka, Z.; Scheiner, S. Structure, Energetics and Vibrational Spectrum of H_2O-HCl. *J. Chem. Phys.* **1987**, *87*, 5928−5936.

(12) Biswal, H. S.; Gloaguen, E.; Loquais, Y.; Tardivel, B.; Mons, M. Strength of NH···S Hydrogen Bonds in Methionine Residues Revealed by Gas-Phase IR/UV Spectroscopy. *J. Phys. Chem. Lett.* **2012**, *3*, 755−759.

(13) Scheiner, S.; Grabowski, S. J.; Kar, T. Influence of Hybridization and Substitution Upon the Properties of the CH··O Hydrogen Bond. *J. Phys. Chem. A* **2001**, *105*, 10607−10612.

(14) Riley, K. E.; Hobza, P. Investigations into the Nature of Halogen Bonding Including Symmetry Adapted Perturbation Theory Analyses. *J. Chem. Theory Comput.* **2008**, *4*, 232−242.

(15) Alkorta, I.; Blanco, F.; Solimannejad, M.; Elguero, J. Competition of Hydrogen Bonds and Halogen Bonds in Complexes of Hypohalous Acids with Nitrogenated Bases. *J. Phys. Chem. A* **2008**, *112*, 10856−10863.

(16) Karpfen, A. Theoretical Characterization of the Trends in Halogen Bonding. In *Halogen Bonding. Fundamentals and Applications*; Metrangolo, P., Resnati, G., Eds.; Springer: Berlin, Germany, 2008; Vol. *126*, pp 1−15.

(17) Hauchecorne, D.; Herrebout, W. A. Experimental Characterization of C−X···Y−C (X = Br, I; Y = F, Cl) Halogen−Halogen Bonds. *J. Phys. Chem. A* **2013**, *117*, 11548−11557.

(18) Zierkiewicz, W.; Michalska, D.; Zeegers-Huyskens, T. Theoretical Investigation of the Conformation, Acidity, Basicity and Hydrogen Bonding Ability of Halogenated Ethers. *Phys. Chem. Chem. Phys.* **2010**, *12*, 13681−13691.

(19) Parisini, E.; Metrangolo, P.; Pilati, T.; Resnati, G.; Terraneo, G. Halogen Bonding in Halocarbon−Protein Complexes: A Structural Survey. *Chem. Soc. Rev.* **2011**, *40*, 2267−2278.

(20) Stephens, S. L.; Walker, N. R.; Legon, A. C. Internal Rotation and Halogen Bonds in CF_3I···NH_3 and CF_3I···$N(CH_3)_3$ Probed by Broadband Rotational Spectroscopy. *Phys. Chem. Chem. Phys.* **2011**, *13*, 20736−20744.

(21) Grabowski, S. J. QTAIM Characteristics of Halogen Bond and Related Interactions. *J. Phys. Chem. A* **2012**, *116*, 1838−1845.

(22) Evangelisti, L.; Feng, G.; Gou, Q.; Grabow, J.-U.; Caminati, W. Halogen Bond and Free Internal Rotation: The Microwave Spectrum of CF_3Cl−Dimethyl Ether. *J. Phys. Chem. A* **2014**, *118*, 579−582.

(23) Riley, K. E.; Murray, J. S.; Fanfrlík, J.; Rezác, J.; Solá, R. J.; Concha, M. C.; Ramos, F. M.; Politzer, P. Halogen Bond Tunability II: The Varying Roles of Electrostatic and Dispersion Contributions to Attraction in Halogen Bonds. *J. Mol. Model.* **2013**, *19*, 4651−4659.

(24) Solimannejad, M.; Malekani, M. Substituent Effects on the Cooperativity of Halogen Bonding. *J. Phys. Chem. A* **2013**, *117*, 5551−5557.

(25) Stone, A. J. Are Halogen Bonded Structures Electrostatically Driven? *J. Am. Chem. Soc.* **2013**, *135*, 7005−7009.

(26) Sanchez-Sanz, G.; Trujillo, C.; Alkorta, I.; Elguero, J. Intramolecular Pnicogen Interactions in Phosphorus and Arsenic Analogues of Proton Sponges. *Phys. Chem. Chem. Phys.* **2014**, *16*, 15900−15909.

(27) Robertson, A. P. M.; Gray, P. A.; Burford, N. Interpnictogen Cations: Exploring New Vistas in Coordination Chemistry. *Angew. Chem., Int. Ed.* **2014**, *53*, 6050−6069.

(28) Scheiner, S. A New Noncovalent Force: Comparison of P···N Interaction with Hydrogen and Halogen Bonds. *J. Chem. Phys.* **2011**, *134*, 094315.

(29) Del Bene, J. E.; Alkorta, I.; Elguero, J. Influence of Substituent Effects on the Formation of P···Cl Pnicogen Bonds or Halogen Bonds. *J. Phys. Chem. A* **2014**, *118*, 2360−2366.

(30) Bauzá, A.; Alkorta, I.; Frontera, A.; Elguero, J. On the Reliability of Pure and Hybrid DFT Methods for the Evaluation of Halogen, Chalcogen, and Pnicogen Bonds Involving Anionic and Neutral Electron Donors. *J. Chem. Theory Comput.* **2013**, *9*, 5201−5210.

(31) Scheiner, S. The Pnicogen Bond: Its Relation to Hydrogen, Halogen, and Other Noncovalent Bonds. *Acc. Chem. Res.* **2013**, *46*, 280−288.

(32) Grabowski, S. J. σ-Hole Bond Versus Hydrogen Bond: From Tetravalent to Pentavalent N, P, and As Atoms. *Chem.—Eur. J.* **2013**, *19*, 14600−14611.
(33) Zahn, S.; Frank, R.; Hey-Hawkins, E.; Kirchner, B. Pnicogen Bonds: A New Molecular Linker? *Chem.—Eur. J.* **2011**, *17*, 6034−6038.
(34) Moilanen, J.; Ganesamoorthy, C.; Balakrishna, M. S.; Tuononen, H. M. Weak Interactions between Trivalent Pnictogen Centers: Computational Analysis of Bonding in Dimers $X_3E\cdots EX_3$ (E = Pnictogen, X = Halogen). *Inorg. Chem.* **2009**, *48*, 6740−6747.
(35) Adhikari, U.; Scheiner, S. Comparison of P···D (D = P,N) with Other Noncovalent Bonds in Molecular Aggregates. *J. Chem. Phys.* **2011**, *135*, 184306.
(36) Bauzá, A.; Quiñonero, D.; Deyà, P. M.; Frontera, A. Halogen Bonding Versus Chalcogen and Pnicogen Bonding: A Combined Cambridge Structural Database and Theoretical Study. *CrystEngComm* **2013**, *15*, 3137−3144.
(37) Iwaoka, M.; Isozumi, N. Hypervalent Nonbonded Interactions of a Divalent Sulfur Atom. Implications in Protein Architecture and the Functions. *Molecules* **2012**, *17*, 7266−7283.
(38) Sánchez-Sanz, G.; Trujillo, C.; Alkorta, I.; Elguero, J. Intermolecular Weak Interactions in Htexh Dimers (X = O, S, Se, Te): Hydrogen Bonds, Chalcogen−Chalcogen Contacts and Chiral Discrimination. *ChemPhysChem* **2012**, *13*, 496−503.
(39) Sanz, P.; Mó, O.; Yáñez, M. Characterization of Intramolecular Hydrogen Bonds and Competitive Chalcogen−Chalcogen Interactions on the Basis of the Topology of the Charge Density. *Phys. Chem. Chem. Phys.* **2003**, *5*, 2942−2947.
(40) Esseffar, M. H.; Herrero, R.; Quintanilla, E.; Dávalos, J. Z.; Jiménez, P.; Abboud, J.-L. M.; Yáñez, M.; Mó, O. Activation of the Disulfide Bond and Chalcogen−Chalcogen Interactions: An Experimental (FTICR) and Computational Study. *Chem.—Eur. J.* **2007**, *13*, 1796−1803.
(41) Iwaoka, M.; Takemoto, S.; Tomoda, S. Statistical and Theoretical Investigations on the Directionality of Nonbonded S···O Interactions. Implications for Molecular Design and Protein Engineering. *J. Am. Chem. Soc.* **2002**, *124*, 10613−10620.
(42) Azofra, L. M.; Scheiner, S. Complexation of n SO_2 Molecules (*n* = 1,2,3) with Formaldehyde and Thioformaldehyde. *J. Chem. Phys.* **2014**, *140*, 034302.
(43) Fanfrlík, J.; Přáda, A.; Padělková, Z.; Pecina, A.; Macháček, J.; Lepšík, M.; Holub, J.; Růžička, A.; Hnyk, D.; Hobza, P. The Dominant Role of Chalcogen Bonding in the Crystal Packing of 2d/3d Aromatics. *Angew. Chem., Int. Ed.* **2014**, *53*, 10139−10142.
(44) Adhikari, U.; Scheiner, S. Sensitivity of Pnicogen, Chalcogen, Halogen and H-Bonds to Angular Distortions. *Chem. Phys. Lett.* **2012**, *532*, 31−35.
(45) Adhikari, U.; Scheiner, S. The S···N Noncovalent Interaction: Comparison with Hydrogen and Halogen Bonds. *Chem. Phys. Lett.* **2011**, *514*, 36−39.
(46) Rosenfield, R. E.; Parthasarathy, R.; Dunitz, J. D. Directional Preferences of Nonbonded Atomic Contacts with Divalent Sulfur. 1. Electrophiles and Nucleophiles. *J. Am. Chem. Soc.* **1977**, *99*, 4860−4862.
(47) Burling, F. T.; Goldstein, B. M. Computational Studies of Nonbonded Sulfur-Oxygen and Selenium-Oxygen Interactions in the Thiazole and Selenazole Nucleosides. *J. Am. Chem. Soc.* **1992**, *114*, 2313−2320.
(48) Werz, D. B.; Gleiter, R.; Rominger, F. Nanotube Formation Favored by Chalcogen-Chalcogen Interactions. *J. Am. Chem. Soc.* **2002**, *124*, 10638−10639.
(49) Jablonski, M. Energetic and Geometrical Evidence of Nonbonding Character of Some Intramolecular Halogen···Oxygen and Other Y···Y Interactions. *J. Phys. Chem. A* **2012**, *116*, 3753−3764.
(50) Bleiholder, C.; Werz, D. B.; Koppel, H.; Gleiter, R. Theoretical Investigations on Chalcogen-Chalcogen Interactions: What Makes These Nonbonded Interactions Bonding? *J. Am. Chem. Soc.* **2006**, *128*, 2666−2674.
(51) Esrafili, M.; Mohammadian-Sabet, F.; Solimannejad, M. A Theoretical Evidence for Mutual Influence between S···N(C) and Hydrogen/Lithium/Halogen Bonds: Competition and Interplay between Π-Hole and Σ-Hole Interactions. *Struct. Chem.* **2014**, *25*, 1197−1205.
(52) George, J.; Deringer, V. L.; Dronskowski, R. Cooperativity of Halogen, Chalcogen, and Pnictogen Bonds in Infinite Molecular Chains by Electronic Structure Theory. *J. Phys. Chem. A* **2014**, *118*, 3193−3200.
(53) Sánchez-Sanz, G.; Alkorta, I.; Elguero, J. Theoretical Study of the HXYH Dimers (X, Y = O, S, Se). Hydrogen Bonding and Chalcogen−Chalcogen Interactions. *Mol. Phys.* **2011**, *109*, 2543−2552.
(54) Smith, G. L.; Mercier, H. P. A.; Schrobilgen, G. J. Ennobling an Old Molecule: Thiazyl Trifluoride ($N{\equiv}SF_3$), a Versatile Synthon for Xe−N Bond Formation. *Inorg. Chem.* **2011**, *50*, 12359−12373.
(55) Umemoto, T.; Singh, R. P.; Xu, Y.; Saito, N. Discovery of 4-*tert*-Butyl-2,6-dimethylphenylsulfur Trifluoride as a Deoxofluorinating Agent with High Thermal Stability as Well as Unusual Resistance to Aqueous Hydrolysis, and Its Diverse Fluorination Capabilities Including Deoxofluoro-Arylsulfinylation with High Stereoselectivity. *J. Am. Chem. Soc.* **2010**, *132*, 18199−18205.
(56) Grunwell, J. R.; Dye, S. L. Novel Generation of Benzonitrile-N-Sulfide. *Tetrahedron Lett.* **1975**, *16*, 1739−1740.
(57) Patel, N. R.; Kirchmeier, R. L.; Shreeve, J. n. M. Reactions of Per- and Polyfluorinated Amines with Sulfur Compounds. *Inorg. Chem.* **1994**, *33*, 4403−4406.
(58) Goettel, J. T.; Kostiuk, N.; Gerken, M. The Solid-State Structure of SF_4: The Final Piece of the Puzzle. *Angew. Chem.* **2013**, *125*, 8195−8198.
(59) Frisch, M. J.; Trucks, G. W.; Schlegel, H. B.; Scuseria, G. E.; Robb, M. A.; Cheeseman, J. R.; Scalmani, G.; Barone, V.; Mennucci, B.; Petersson, G. A.; et al. *Gaussian 09*, revision B.01; Gaussian, Inc.: Wallingford, CT, 2009.
(60) Chen, Y.; Yao, L.; Lin, X. Theoretical Study of $(FH_2X)_n{\cdot}Y$ (X = P and As, *n* = 1−4, Y = F^-, Cl^-, Br^-, I^-, NO_3^- and SO_4^{2-}): The Possibility of Anion Recognition Based on Pnicogen Bonding. *Comput. Theor. Chem.* **2014**, *1036*, 44−50.
(61) Esrafili, M. D.; Fatehi, P.; Solimannejad, M. Mutual Interplay between Pnicogen Bond and Dihydrogen Bond in HMH···HCN···PH_2X Complexes (M = Be, Mg, Zn; X = H, F, Cl). *Comput. Theor. Chem.* **2014**, *1034*, 1−6.
(62) Hauchecorne, D.; Nagels, N.; van der Veken, B. J.; Herrebout, W. A. C−X···π Halogen and C−H···π Hydrogen Bonding: Interactions of CF_3X (X = Cl, Br, I or H) with Ethene and Propene. *Phys. Chem. Chem. Phys.* **2012**, *14*, 681−690.
(63) Wu, W.; Lu, Y.; Liu, Y.; Li, H.; Peng, C.; Liu, H.; Zhu, W. Weak Energetic Effects between X−π and X−N Halogen Bonds: CSD Search and Theoretical Study. *Chem. Phys. Lett.* **2013**, *582*, 49−55.
(64) Kerdawy, A. E.; Murray, J. S.; Politzer, P.; Bleiziffer, P.; Heßelmann, A.; Görling, A.; Clark, T. Directional Noncovalent Interactions: Repulsion and Dispersion. *J. Chem. Theory Comput.* **2013**, *9*, 2264−2275.
(65) Ji, W.-Y.; Xia, X.-L.; Ren, X.-H.; Wang, F.; Wang, H.-J.; Diao, K.-S. The Non-Covalent Bindings of CF_2Cl_2 with NO and SO_2. *Struct. Chem.* **2013**, *24*, 49−54.
(66) Boys, S. F.; Bernardi, F. The Calculation of Small Molecular Interactions by the Differences of Separate Total Energies. Some Procedures with Reduced Errors. *Mol. Phys.* **1970**, *19*, 553−566.
(67) Bulat, F.; Toro-Labbé, A.; Brinck, T.; Murray, J.; Politzer, P. Quantitative Analysis of Molecular Surfaces: Areas, Volumes, Electrostatic Potentials and Average Local Ionization Energies. *J. Mol. Model.* **2010**, *16*, 1679−1691.
(68) Moszynski, R.; Wormer, P. E. S.; Jeziorski, B.; van der Avoird, A. Symmetry-Adapted Perturbation Theory of Nonadditive Three-Body Interactions in van der Waals Molecules. I. General Theory. *J. Chem. Phys.* **1995**, *103*, 8058−8074.
(69) Szalewicz, K.; Jeziorski, B. Symmetry-Adapted Perturbation Theory of Intermolecular Interactions. In *Molecular Interactions. From*

Van der Waals to Strongly Bound Complexes; Scheiner, S., Ed.; Wiley: New York, 1997; pp 3−43.
(70) Werner, H.-J.; Knowles, P. J.; Manby, F. R.; Schütz, M.; Celani, P.; Knizia, G.; Korona, T.; Lindh, R.; Mitrushenkov, A.; Rauhut, G.; et al. *MOLPRO*, version 2006; Cardiff University: Cardiff, U.K., 2010.
(71) Reed, A. E.; Weinhold, F.; Curtiss, L. A.; Pochatko, D. J. Natural Bond Orbital Analysis of Molecular Interactions: Theoretical Studies of Binary Complexes of HF, H_2O, NH_3, N_2, O_2, F_2, CO and CO_2 with HF, H_2O, and NH_3. *J. Chem. Phys.* **1986**, *84*, 5687−5705.
(72) Reed, A. E.; Curtiss, L. A.; Weinhold, F. Intermolecular Interactions from a Natural Bond Orbital, Donor-Acceptor Viewpoint. *Chem. Rev.* **1988**, *88*, 899−926.
(73) Goettel, J. T.; Chaudhary, P.; Hazendonk, P.; Mercier, H. P. A.; Gerken, M. $SF_4{\cdot}N(C_2H_5)_3$: The First Conclusively Characterized SF_4 Adduct with an Organic Base. *Chem. Commun.* **2012**, *48*, 9120−9122.
(74) Clark, T.; Murray, J. S.; Lane, P.; Politzer, P. Why Are Dimethyl Sulfoxide and Dimethyl Sulfone Such Good Solvents? *J. Mol. Model.* **2008**, *14*, 689−697.